EUROPHYSICS LETTERS 10 November 1994

Europhys. Lett., 28 (5), pp. 335-340 (1994)

Stability and Band Gap Constancy of Boron Nitride Nanotubes.

X. BLASE, A. RUBIO, S. G. LOUIE and M. L. COHEN

Department of Physics, University of California at Berkeley
Materials Sciences Division, Lawrence Berkeley Laboratory - Berkeley, CA 94720, USA

(received 6 June 1994; accepted 4 October 1994)

PACS. 71.25T – Band structure of crystalline semiconductor compounds and insulators.
PACS. 71.10 – General theories and computational techniques.
PACS. 36.20K – Electronic structure and spectra.

Abstract. – Extensive LDA and quasi-particle calculations have been performed on boron nitride (BN) single-wall and multi-wall nanotubes. Strain energies are found to be smaller for BN nanotubes than for carbon nanotubes of the same radius, owing to a buckling effect which stabilizes the BN tubular structure. For tubes larger than 9.5 Å in diameter, the lowest conduction band is predicted to be free-electron–like with electronic charge density localized inside the tube. For these tubes, this band is at constant energy above the top of the valence band. Consequently, contrarily to carbon nanotubes, single- and multi-wall BN nanotubes are constant-band-gap materials, independent of their radius and helicity. In addition, we expect them to exhibit remarkable properties under n-type doping.

In a recent paper [1], the existence of boron nitride (BN) nanotubes was proposed. Based upon similarities between carbon and BN-based materials, it was suggested that these tubes may be stable and their electronic properties were studied within an empirical Tight-Binding (TB) approach. However, because of the lack of a total-energy calculation scheme within TB for BN-based materials, no evidence for the stability of BN nanotubes was given and the calculations were restricted to tubes with the «ideal» geometry given by rolling a single sheet of hexagonal BN into a tubular shape. In addition, as shown recently for carbon nanotubes [2], the large curvature of small tubes may induce strong hybridization effects which strongly modify the band structure given by a standard s-p Slater-Koster TB scheme.

In this work, we carry out *ab initio* pseudopotential local-density-functional (LDA) calculations to study from first principles the structural stability of this novel form of BN. Further, we study the electronic properties of BN nanotubes, both within LDA and within a more accurate quasi-particle approach. The electronic properties of multi-wall BN tubes are also investigated. The calculation of the quasi-particle energies is performed using a self-energy approach [3], based on the Hedin's GW approximation [4]. Technical details for the quasi-particle calculation will be described elsewhere [5]. Pseudopotentials and electron wave functions are expanded in a plane-wave basis. The energy cut-off for the electronic wave functions is set at $E_{\text{cut}} = 45$ Ry to converge both total energies and eigenvalues. Boron

and nitrogen pseudopotentials are generated following the Kleinman and Bylander procedure [6]. The calculations are carried out in a supercell geometry with a hexagonal array of tubes. The closest distance between atoms on neighboring tubes is set at 5 Å. Within this geometry, tube-tube interactions are negligible.

By minimizing both stress and Hellmann-Feynman forces, we determine first the equilibrium geometry for $(n, 0)$ and (n, n) tubes with diameters ranging from 4 to 12 Å (index notations for the tubes refer to the convention of ref. [7, 8] as defined for graphitic nanotubes). The main relaxation effect is a buckling of the boron-nitrogen bond, together with a small contraction of the bond length ($\sim 1\%$). In the minimum energy structure, all the boron atoms are arranged in one cylinder and all the nitrogen atoms in a larger concentric one. Due to charge transfer from boron to nitrogen, the buckled tubular structure forms a dipolar shell. The distance between the inner «B-cylinder» and the outer «N-cylinder» is, at constant radius, mostly independent of tube helicity and decreases from 0.2 a.u. for the (4, 4) tube to 0.1 a.u. for the (8, 8) tube. As a result of this buckling, each boron atom is virtually located on the plane formed by its three neighboring nitrogen atoms so that the sp^2 environment for the boron atom in the planar hexagonal structure is restored (at most, the $\widehat{NBN}$ angles differ from 120° by 0.2% for the smallest tube). This tendency for threefold coordinated column-III atoms to seek the 120° bond angle is extremely strong. For example, it explains the atomic relaxation of the (110) and (111)-2 × 2 surfaces of GaAs and other III-V compounds [9]. On the other hand, the $\widehat{BNB}$ angles approach the value of the bond angle of the s^2p^3 geometry. This is also consistent with previous calculations performed on small $B_{12}N_{12}$ clusters [10] where a similar buckling of the BN bond was observed for a monocyclic ring structure. Buckling and bond length reduction induce a contraction of the tube along its axial direction by a maximum of 2% for the smallest tube studied.

Energies per atom for the relaxed tubes are plotted in fig. 1 as a function of the tube diameter. The zero of energy is taken to be the energy per atom of an isolated hexagonal BN sheet. On the same graph, the energy per carbon atom above the graphite sheet energy is represented. As for graphitic tubes, BN tube energies follow the classical $1/R^2$ strain law, where R is the average radius of each tube. However, for the same radius, the calculated strain energy of BN nanotubes is smaller than the strain energy of graphitic tubes. This is

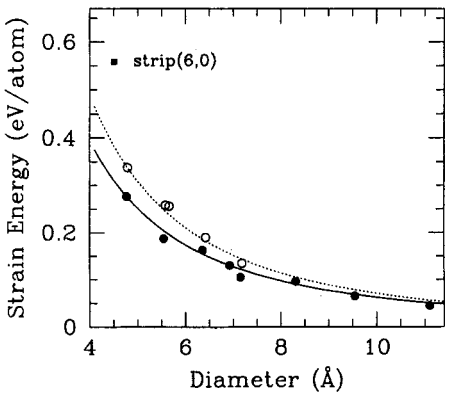

Fig. 1. – Total energy of nanotubes in eV/atom as a function of tube diameter (in Å). The black circles represent the BN nanotube energies above the energy of an isolated hexagonal BN sheet. The opened circles represent the graphite nanotubes energies above the energy per atom of an isolated graphite sheet. The solid and dashed lines are guides to the eye. The energy of the strip corresponding to the (4, 4) BN tube is given by the filled square.

related mostly to the buckling effect which reduces significantly the occupied band energy in the case of the BN compounds. Therefore, it is energetically more favorable to fold a hexagonal BN sheet onto a nanotube geometry than to form a carbon nanotube from a graphite sheet. Based on the existence of carbon nanotubes, we conclude that BN nanotubes are metastable structures.

We also address the question of stability of a small tube *vs.* opening into a strip of hexagonal BN [11]. We performed total-energy calculations for the strip corresponding to the small tube (6,0), allowing complete relaxation of the strip geometry. As shown in fig. 1 (filled square), the strip is less stable than the corresponding tube. As for carbon nanotubes, BN nanotubes with a radius larger than 4 Å are stable with respect to a strip.

Because of its larger ionicity, a hexagonal BN sheet is a large-gap semiconductor in contrast to graphite which is semi-metallic. Consequently, on the basis of a band-folding analysis [7,8], BN nanotubes are large-gap semiconductors, with direct gap at Γ for $(n, 0)$ tubes and indirect gap for (n, n) tubes. However, strong hybridization effects can occur because of curvature of the tubes which may strongly modify the band structure given by the band-folding analysis. As for carbon nanotubes [2], the present *ab initio* LDA calculations show that for small $(n, 0)$ tubes, a π^*-σ^* hybridized state significantly reduces the gap predicted by the band-folding analysis. Consistent with its carbon analog, this state is at Γ with wave function localized outside the tube. It corresponds to the hexagonal BN π^* state at K which is folded onto the tube Γ-point when rolling the BN sheet onto a $(n, 0)$ tube. Once folded, this state lowers its energy by interacting with the σ^* state at Γ. However, the consequences of the energy lowering of this state within LDA are less important than that in the case of carbon nanotubes since $(n, 0)$ BN tubes remain large-gap semiconductors with a LDA minimum of 2.5 eV for the (6,0) tube. With decreasing tube curvature, the hybridization effects are less important. For $(n, 0)$ tubes such that $n > 12$ (which corresponds to a diameter larger than 9.5 Å), the hybrid state does not play any role in determining the gap of the BN tubes.

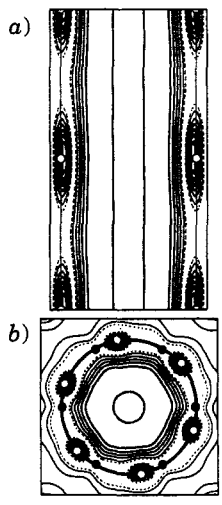

Fig. 2. – Contour plot of the charge density corresponding to the bottom of the conduction band state at Γ for the (6, 6) BN nanotube. *a*) Plot in a plane containing the axis of the tube and N atoms. N atoms are indicated by empty circles. *b*) Plot in a plane perpendicular to the tube axis containing B and N atoms. B atoms are represented by filled circles. The minimum contour line (dashed line) corresponds to $0.04e/(\text{a.u.})^3$ and the maximum to $0.026e/(\text{a.u.})^3$ (thicker black line). We draw the two concentric B- and N-cylinders to stress the buckling relaxation. The parabolic dispersion of the NFE state can be described through the band-folding picture (see text).

For (n, n) tubes, the key feature is the bottom of the conduction band at Γ. For all (n, n) tubes studied, this state is within LDA located at around 4 eV above the top of the valence band, independent of tube radius. In addition, this state is uniquely characterized by a remarkable charge density distribution. As shown in fig. 2 for the (6,6) tube, this state yields a nearly constant charge density filling the interior of the tube. Since in this region the tube potential is constant, this state has a nearly-free–like electron (NFE) behavior. The effective mass at Γ for this NFE band is calculated to be $m^* = 1 \pm 0.1\ m_e$ for all tubes, where m_e is the free-electron mass.

In a band-folding analysis, this NFE state corresponds to the bottom of the conduction band at Γ for hexagonal BN. This is shown in fig. 3 where we compare the LDA band structure for the BN (4, 4) tube to the LDA hexagonal BN band structure. In this calculation, the distance between two BN planes is set to the (4, 4) tube diameter. We selected directions in the hexagonal Brillouin zone (BZ) which, in a band-folding analysis, would yield the tube top of the valence and bottom of the conduction bands. As one can see, the bottom of the conduction band is very similar in both structures, with hardly any modification in position and shape around the center of the zone. For hexagonal BN, the charge density of the state at the bottom of the conduction band is located on the nitrogen atoms and in the interplanar region. It is the analog of the σ^* state at Γ in graphite [12] and has been referred to as the interlayer state.

Since the NFE tube state at Γ is the image of the interlayer state in the band-folding mapping, it exists in all tubes independently of their helicity. We note that the NFE state is very constant in energy and does not hybridize with curvature: this is because its wave function does not overlap with those of other states which are mostly localized on the tube wall. This explains that, even for the smaller tubes, the LDA band gap is stabilized at around 4 eV, except for the few $(n, 0)$ tubes with $n \leqslant 12$. Even for these tubes, for which the π^*-σ^* hybrid state forms the bottom of the conduction band, the NFE state is within LDA localized at 4 eV above the top of the valence band. We study also the band structure of two concentric tubes (in the case of carbon, most graphitic «needles» are formed of concentric tubes). We select the (4, 4) and (9, 9) tubes. The difference between their radii is comparable to the van der Waals equilibrium distance between two layers in bulk hexagonal BN. Tube-tube

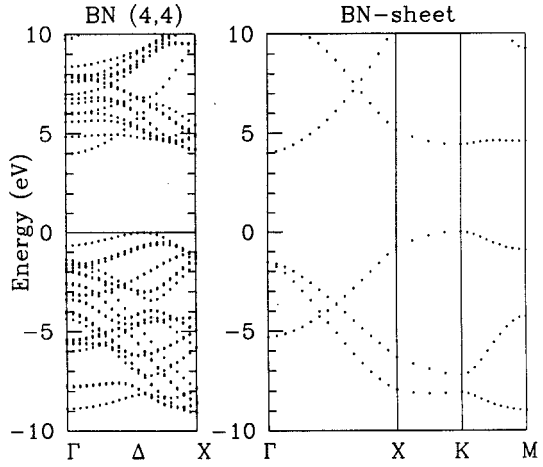

Fig. 3. – Band structure of the BN (4, 4) tube compared to hexagonal BN band structure plotted along high-symmetry directions of the 2D hexagonal Brillouin zone. X is between Γ and K with $\Gamma X = (3/4)\,\Gamma K$. Energies are in eV and the zero of energy is at the top of the valence band for both structures.

interaction hardly modifies the energy and wave function of the innermost tube NFE state, which remains the bottom of the conduction band at 4 eV above the top of the valence band. We emphasize therefore that for all BN tubes (except the $(n, 0)$ tubes with $n \leqslant 12$) the band gap is stabilized around 4 eV (LDA value) and the bottom of the conduction band is a NFE-like state.

Since a band-folding analysis correctly describes the band structure of most BN tubes, we perform a more accurate description of the electronic properties of these tubes by studying within a quasi-particle formalism the electronic band structure of hexagonal boron-nitride compounds. Several structures are studied which are composed of periodically repeated layers of hexagonal BN sheets, with an interlayer distance varying from $d = 5.5$ Å (diameter of the (4, 4) tube) to $d = 13.5$ Å. By including layer-layer interactions, we investigate the effects of the overlap of orbitals inside small tubes and of tube-tube interactions in multi-wall structures. For $d = 13.5$ Å, two neighboring layers do not interact. Therefore, the corresponding band structure can be used to obtain the band structure of large-diameter BN tubes. For all these layered structures, the quasi-particle band gap is indirect between the top of the valence band at M and the bottom of the conduction band at Γ. The calculated band gap is very stable around 5.5 eV for all interlayer distances d. This is in excellent agreement with the experimental value of 5.8 eV for bulk hexagonal boron nitride [13]. Therefore, the quasi-particle calculation confirms the physical picture given by the LDA approach; single-wall and multi-wall BN nanotubes are nearly-constant-gap materials with a band gap around 5.5 eV (quasi-particle value). In addition, the lowest occupied state is a NFE-like state with charge density localized inside the tube.

As discussed above, for bulk BN, the interlayer state has maximum and nearly uniform charge density in the vacuum region between BN layers. For $d = 13.5$ Å, the «interlayer state» does not overlap with the one of a neighboring layer. However, it remains localized in the vacuum region with a maximum charge density at ~ 2 Å away from the corresponding BN plane. Consequently, for very large tubes, we expect the charge density for the NFE state at Γ to be localized in a region at about 2 Å interior at the tube wall and to remain NFE-like. We remark that the interlayer state described here does not exist in a usual TB approach based on a minimum ($3s$, $3p_x$, $3p_y$, $3p_z$) basis. Therefore, even in the limit of large nanotubes, for which hybridization effects are negligible, a simple TB approach would not describe correctly the nature of the BN tube gaps. This is contrary to the case of carbon nanotubes where TB and LDA results agree for large tubes. In the case of graphite, the interlayer state within LDA is 2 eV above the bottom of the conduction band, so that this NFE state is at higher energy in the conduction bands and does not play any role in the metallicity and doping properties of the carbon nanotubes.

In conclusion, we find that the wrapping of the planar hexagonal structure onto the tube geometry is comparable to slightly more favorable for BN tubes than carbon nanotubes. This is mostly related to a buckling effect which stabilizes the BN tubular structure. The BN nanotubes are predicted to be wide-gap semiconductors with a value of ~ 5.5 eV, independently of their radius and helicity. This insensitivity of the BN tube band gap *vs.* variation in radius, helicity and coaxial arrangement may be of crucial importance for technological applications because samples containing many different sizes and structures, single-wall or multi-walls tubes, could be grown with predictable electronic properties [1]. This constant-gap value is related to the bottom of the conduction band state which has a

---

[1] We note that of all the tubes studied containing C, B and N in various proportions, BN nanotubes are the only ones to exhibit such a constant gap. This should facilitate greatly the experimental characterization of pure BN nanotubes. For a study of BC_3 and BC_2N nanotubes, see [14].

nearly-free-electron–like behavior with charge density localized inside the tube. We expect this property to have important technological implications particularly in the case of n-type doping.

* * *

This work was supported by National Science Foundation Grant No. DMR-9120269 and by the Director, Office of Energy Research, Office of Basic Energy Sciences, Materials Sciences Division of the US Department of Energy under contract No. DE-AC03-76SF00098. AR was supported by a Fullbright-MEC grant. We would like to thank Drs. D. J. CHADI and Y. MIYAMOTO for helpful discussions. Supercomputer time was provided by the NSF Pittsburgh Supercomputer Center and by the DOE NERSC facility.

REFERENCES

[1] RUBIO A., CORKILL J. L. and COHEN M. L., *Phys. Rev. B*, **49** (1994) 5081. We note that large-size, turbostratic, tubular BN structures had been previously reported to be obtained upon heating of amorphous BN to 1100 °C. See: HAMILTON E. J. M., DOLAN S. E., MANN C. M., COLIJN H. O., MCDONALD C. A. and SHORE S. G., *Science*, **260** (1993) 659.
[2] BLASE X., BENEDICT L. X., SHIRLEY E. L. and LOUIE S. G., *Phys. Rev. Lett.*, **72** (1994) 1878.
[3] HYBERTSEN M. S. and LOUIE S. G., *Phys. Rev. Lett.*, **55** (1985) 1418; *Phys. Rev. B*, **34** (1986) 5390.
[4] HEDIN L. and LUNQVIST S., in *Solid State Physics: Advances in Research and Applications*, edited by F. SEITZ, D. TURNBULL and H. EHRENREICH, Vol. **23** (Academic, New York, N.Y.) 1969.
[5] BLASE X., RUBIO A., LOUIE S. G. and COHEN M. L., submitted to *Phys. Rev. B*.
[6] KLEINMAN L. and BYLANDER D. M., *Phys. Rev. Lett.*, **48** (1982) 1425.
[7] SAITO R., FUJITA M., DRESSELHAUS G. and DRESSELHAUS M. S., *Appl. Phys. Lett.*, **60** (1992) 2204.
[8] HAMADA N., SAWADA S. and OSHIYAMA A., *Phys. Rev. Lett.*, **68** (1992) 1759.
[9] CHADI D. J., private communication.
[10] JENSEN F. and TOFLUND H., *Chem. Phys. Lett.*, **201** (1993) 89.
[11] LUCAS A. A., LAMBIN P. H. and SMALLEY R. E., *J. Phys. Chem. Solids*, **54** (1993) 587.
[12] HOLZWARTH N. A. W., LOUIE S. G. and RABII S., *Phys. Rev. B*, **26** (1982) 5382.
[13] ZUNGER A., KATZIR A. and HALPERIN A., *Phys. Rev. B*, **13** (1974) 5560.
[14] MIYAMOTO Y., RUBIO A., LOUIE S. G. and COHEN M. L., *Phys. Rev. B*, **50** (1994) 4976.